Regular particle acceleration in relativistic jets

G.S.Bisnovatyi-Kogan

Space Research Institute RAN, Moscow
Joint Institute of Nuclear Researches, Dubna

Bonn,
Oct.1, 2004

Objects of different scale and nature in the universe: from young and very old stars to active galactic nuclei show existence of collimated outbursts - jets.

Geometrical sizes of jets lay between parsecs and megaparsecs.

The origin of jets is not well understood and only several mechanisms are proposed.

Theory of jets should answer to the questions

1. of the origin of relativistic particles in outbursts from AGN, where synchrotron emission is observed.

2. Relativistic particles, ejected from the central machine rapidly loose their energy so the problem arises of particle acceleration inside the jet.

Microquasar

GRS 1915+105

Jet ejection

MERLIN 5GHz

Fender (1999)

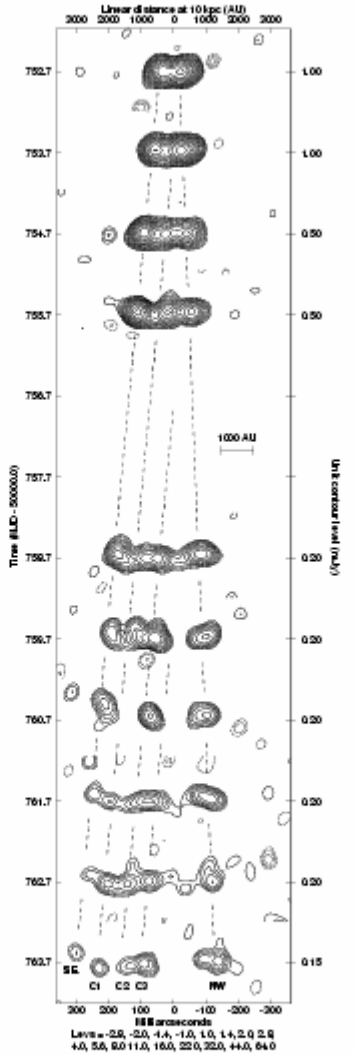

Fig. 2. A sequence of ten epochs of radio imaging of relativistic ejections from the black hole candidate X-ray binary GRS 1915+105 using MERLIN at 5 GHz. The figure has been rotated by 52 degrees to form the montage. Contour levels increase in factors of $\sqrt{2}$ from the unit contour level indicated at the right hand side of each image. Components SE, C1, C2 & C3 are approaching with a mean proper motion of 23.6 ± 0.5 mas d^{-1}. Component NW is receding with a mean proper motion of 10.0 ± 0.5 mas d^{-1} and corresponds to the same ejection event which produced approaching component SE. For an estimated distance to the source of 11 kpc the approaching components have an apparent transverse velocity of 1.5c. Assuming an intrinsically symmetric ejection and the standard model for apparent superluminal motions, we derive an intrinsic bulk velocity for the ejecta of $0.98^{+0.02}_{-0.05}c$ at an angle to the line of sight of 66 ± 2 degrees (at 11 kpc). The ejections occurred after a 20-day 'plateau' during which the X-ray emission was hard and stable and the radio had an inverted spectrum. The first two ejections were punctuated by four days of rapid radio oscillations, indicative of an unstable inner accretion disc being repeatedly ejected [14,38,34,8,16]. The apparent curvature of the jet is probably real, although the cause of the bending is uncertain. A detailed presentation and discussion of these results may be found in [18].

X-ray image of

microquasar

XTE J1550-564(center)

with two jets.

0.3-7 keV

11 March 2002

Chandra

Kaaret et al. (2002)

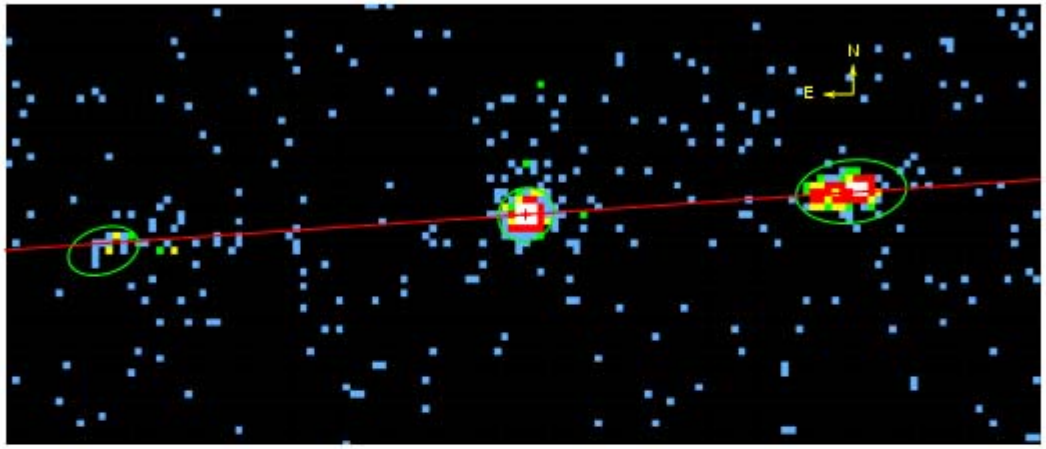

Fig. 1.— X-ray image of XTE J1550–564 for the 0.3–7 keV band taken on 11 March 2002. The color of each pixel represents the number of X-ray counts: black = 0 counts, blue = 1, green = 2, yellow = 3–4, red = 5-20, white = 21-330. The green ellipses are source regions and indicate detection of the western and eastern jets in addition to XTE J1550–564 itself. The red line is the axis of the superluminal jet emission at a position angle of −86.1° (D. Hannikainen, private communication). The arrows indicating north and east are 2″ long.

TABLE 1
X-RAY SOURCES NEAR XTE J1550–564

	Date	RA	DEC	S/N	Counts	Flux	Comment
1	March	15 50 58.66	-56 28 35.2	334.3	1163.4	4.64	XTE J1550–564
	June	15 50 58.66	-56 28 35.2	26.3	54.5	0.31	
2	March	15 50 55.97	-56 28 33.6	122.5	409.1	1.64	Western Jet

X ray image of microquasar **XTE J1550-564** (left) and western jet. Upper panel is from 11 March 2002. Lower panel is from 19 June 2002. **Chandra,** 0.3-7 keV Kaaret et al. (2002)

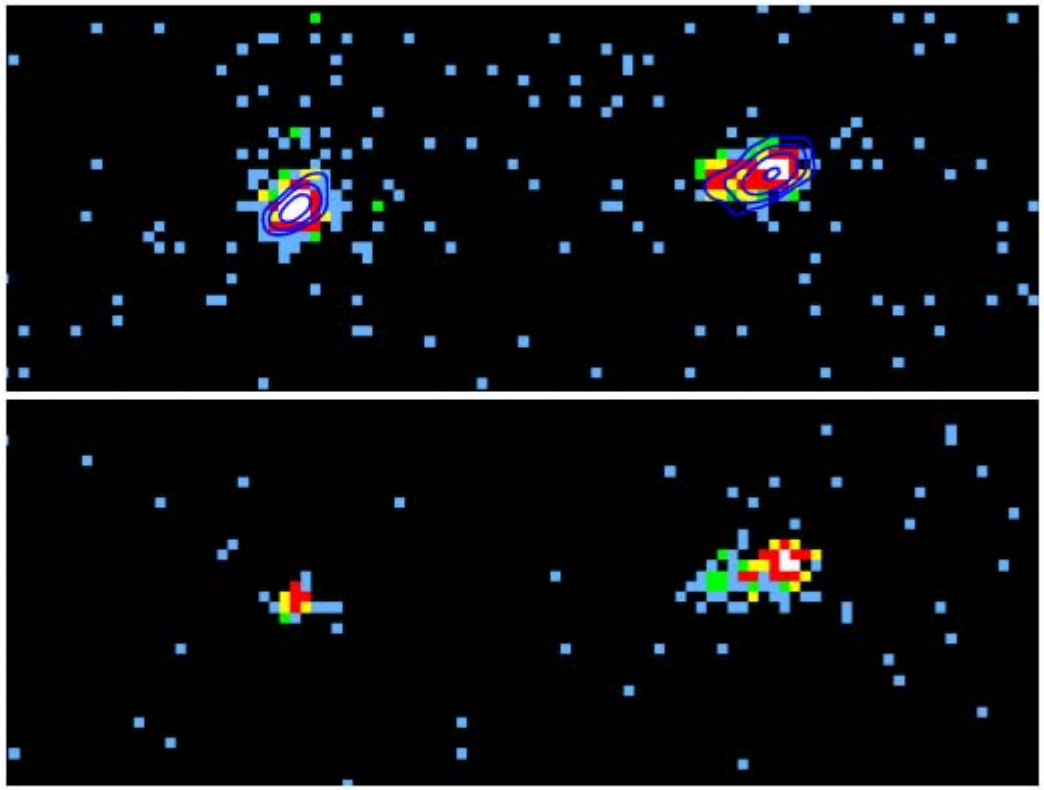

Fig. 3.— X-ray images of XTE J1550–564 (on the left = east) and the western jet (on the right = west). The upper panel is from the 11 March 2002 observation and the lower panel is from the 19 June 2002 observation. The X-ray data are for the 0.3–7 keV band and the color scale is the same as in Fig. 1. The upper panel has with radio contours (dark blue curves) from an observation on 29 January 2002 superimposed. The contour levels are 0.2, 0.4, 0.8, and 1.6 mJy.

Jet in M 87:

Radio: 6 cm (up),
Optical: V-band (middle),
Chandra:
X-ray 0.1-10 keV (down)

Wilson , Yang (2001)

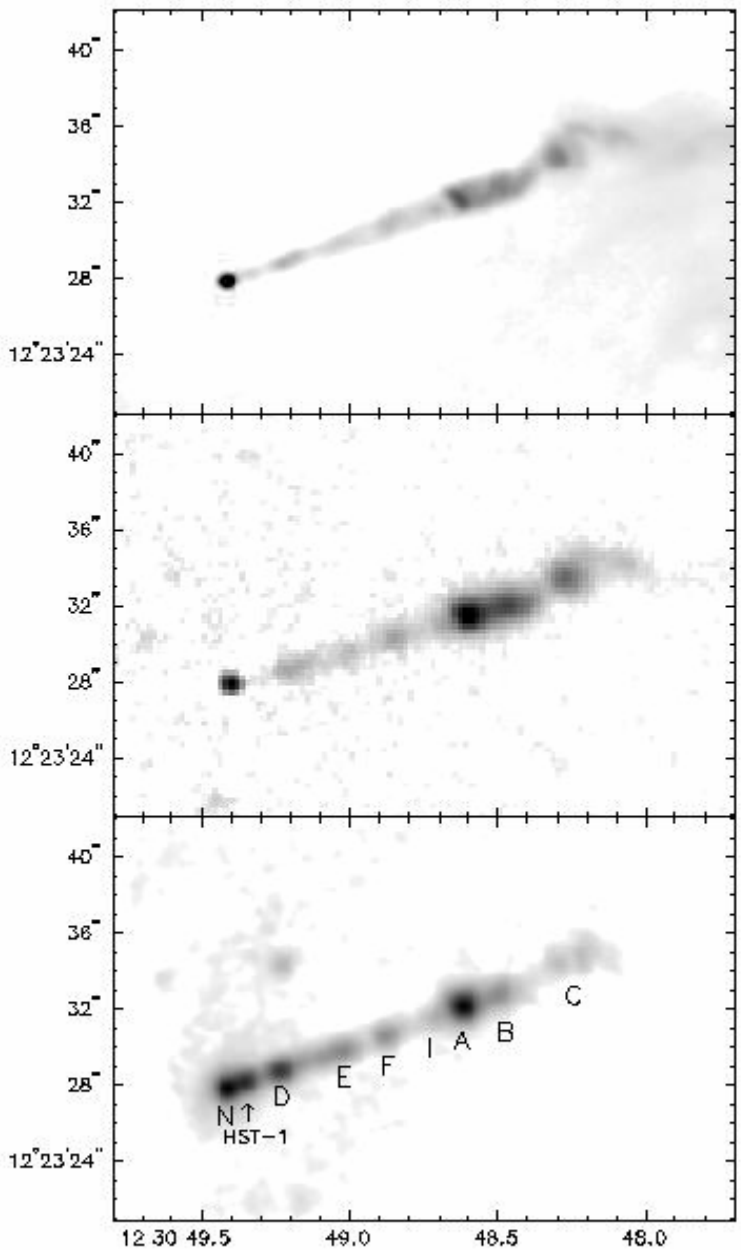

HST

Livio, 2003

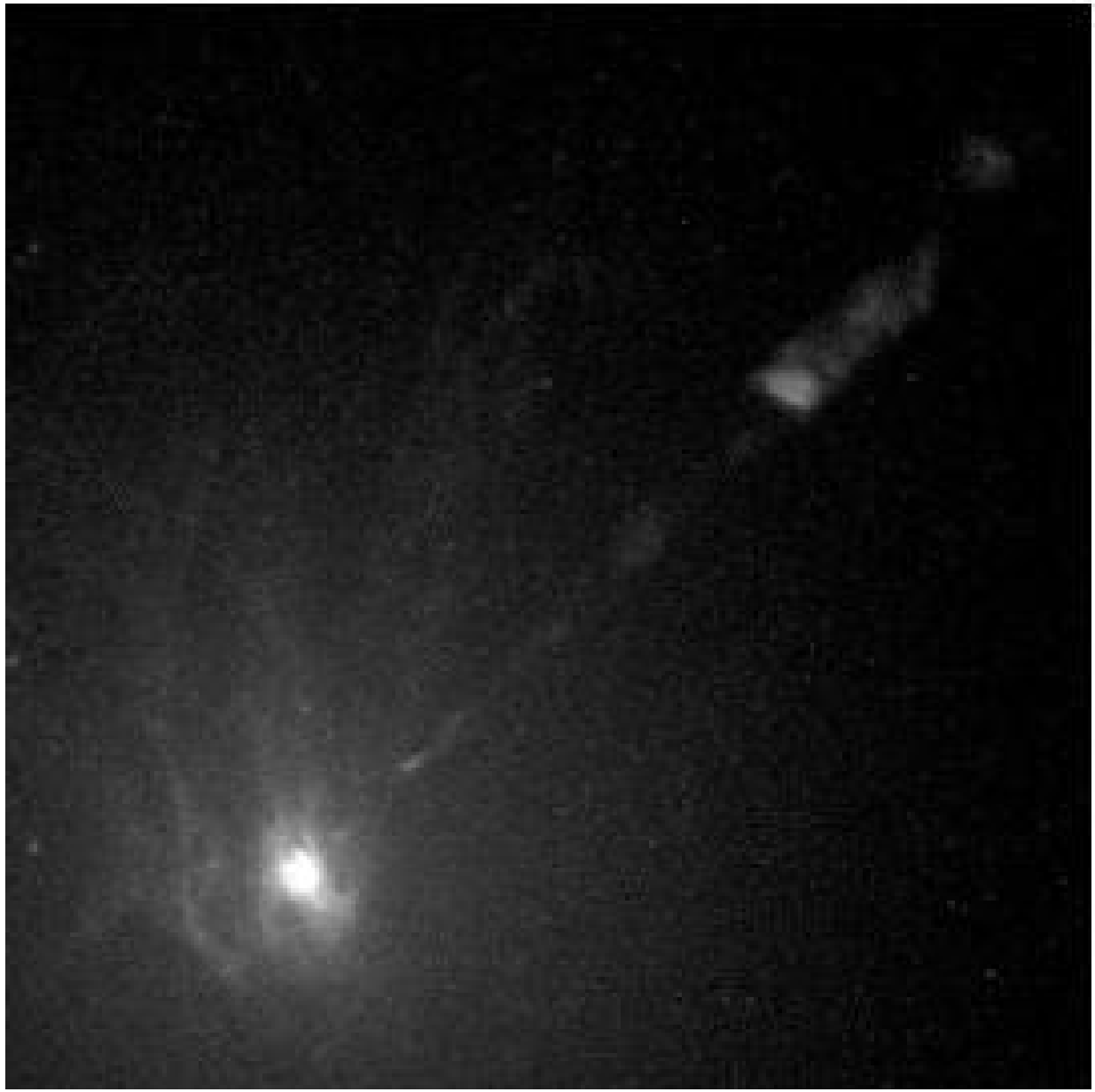

M 87 jet: **Chandra** image, Harris et al. (2003)

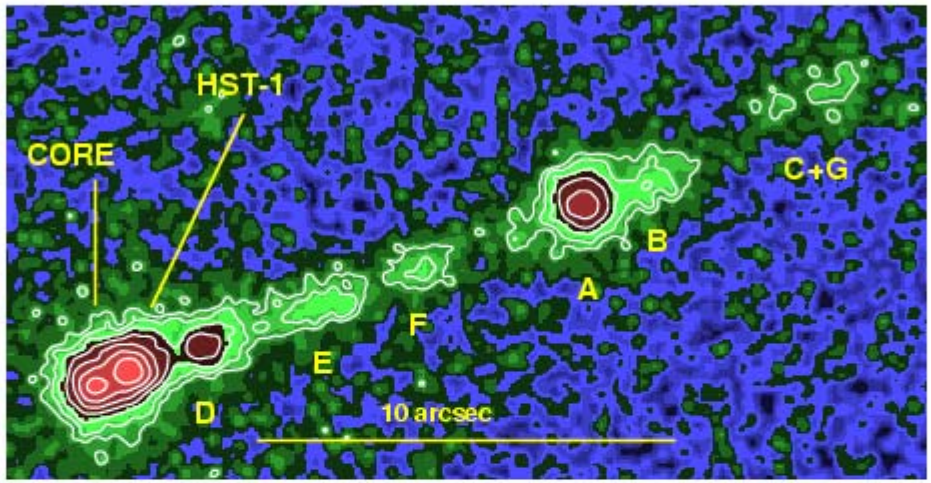

FIG. 1.— Chandra X-ray image of the M87 jet constructed by averaging the data of Wilson & Yang (2002) taken in 2000 July, together with our 5 observations. The contours increase by factors of two in brightness, with the lowest contour level being 1×10^{-16} erg cm^{-2} s^{-1} per pixel in the 0.2 to 6 keV band. Jet features are labelled according to the standard convention and a 10″ scalebar is shown. ACIS pixel randomization has been removed; the data were regridded to a pixel size of 0.0492″; and a Gaussian smoothing function of FWHM=0.25″ was applied.

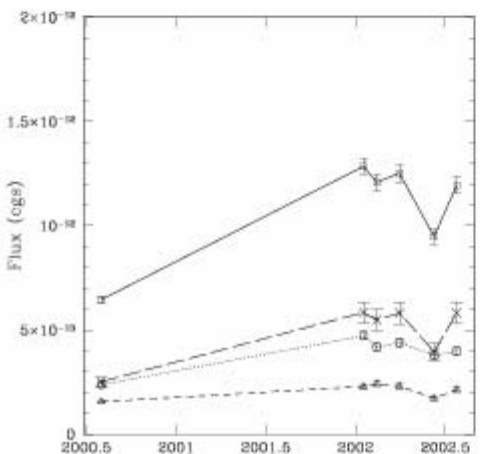

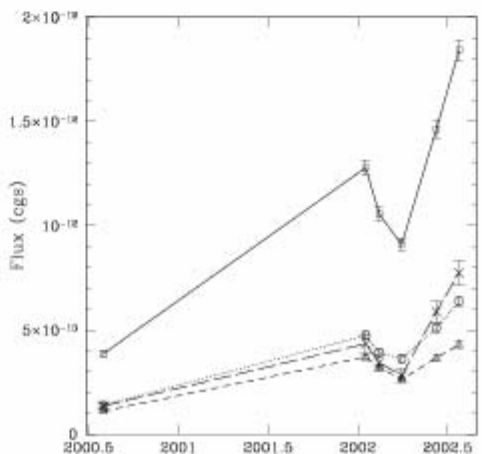

MERLIN map of 3C 273 at 408 MHz resolution: 1.0 arcsec

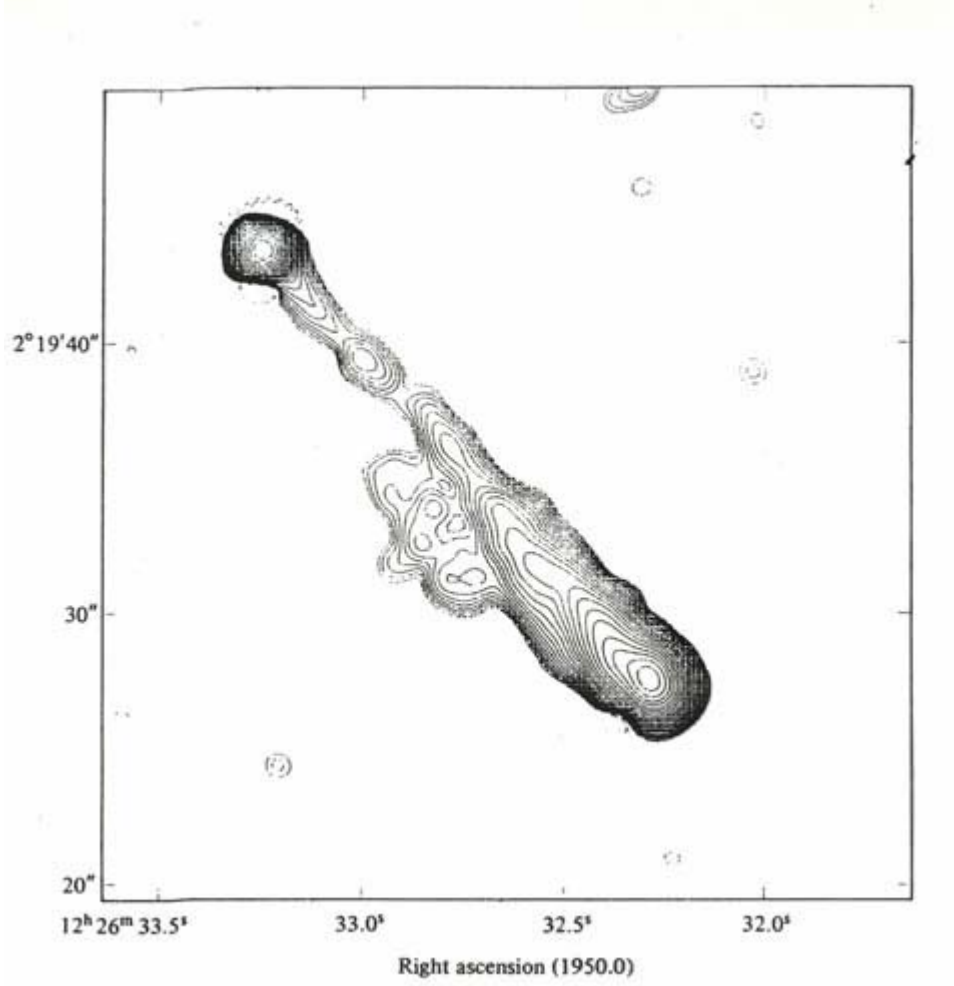

3C 273

Left:

MERLIN, 1.647 GHz.

Middle:

HST(F622W), 6170A.

Right:

Chandra, 0.1 “

Marshall et al. (2000)

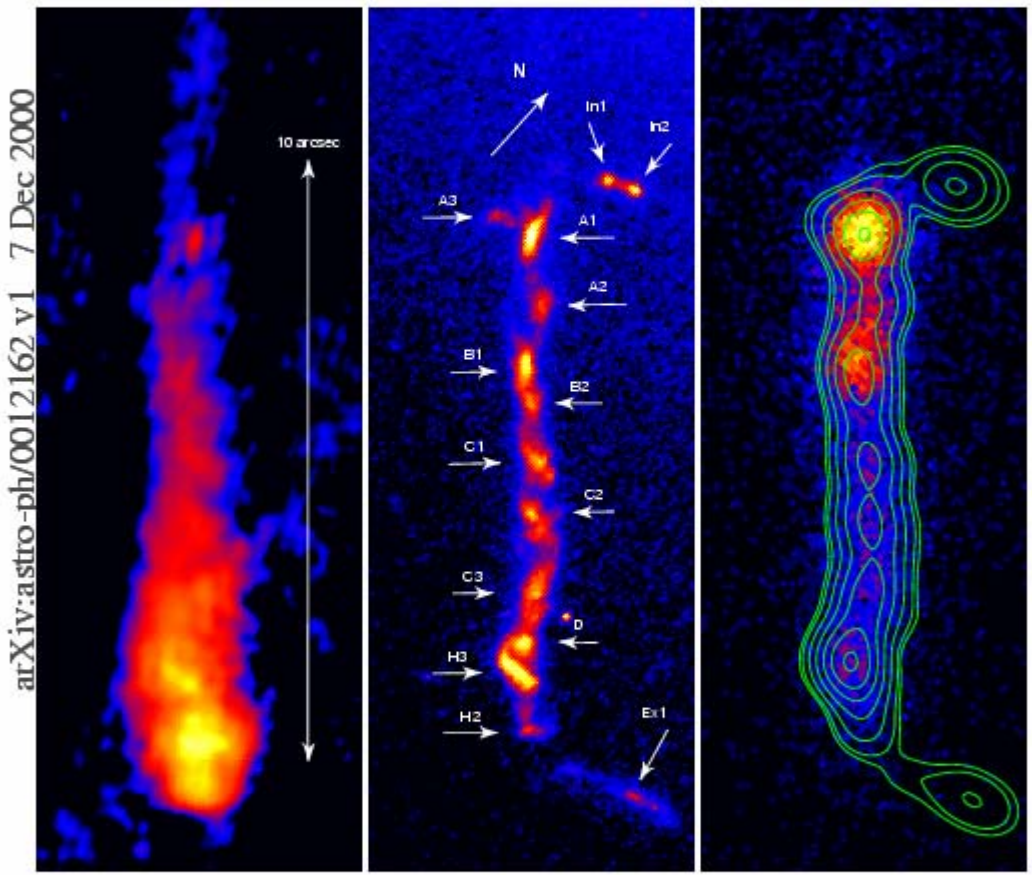

Jet in 3C 273
Chandra
observations

Samburina et al. (2001)

10” is about

22 kpc

Long exposition.

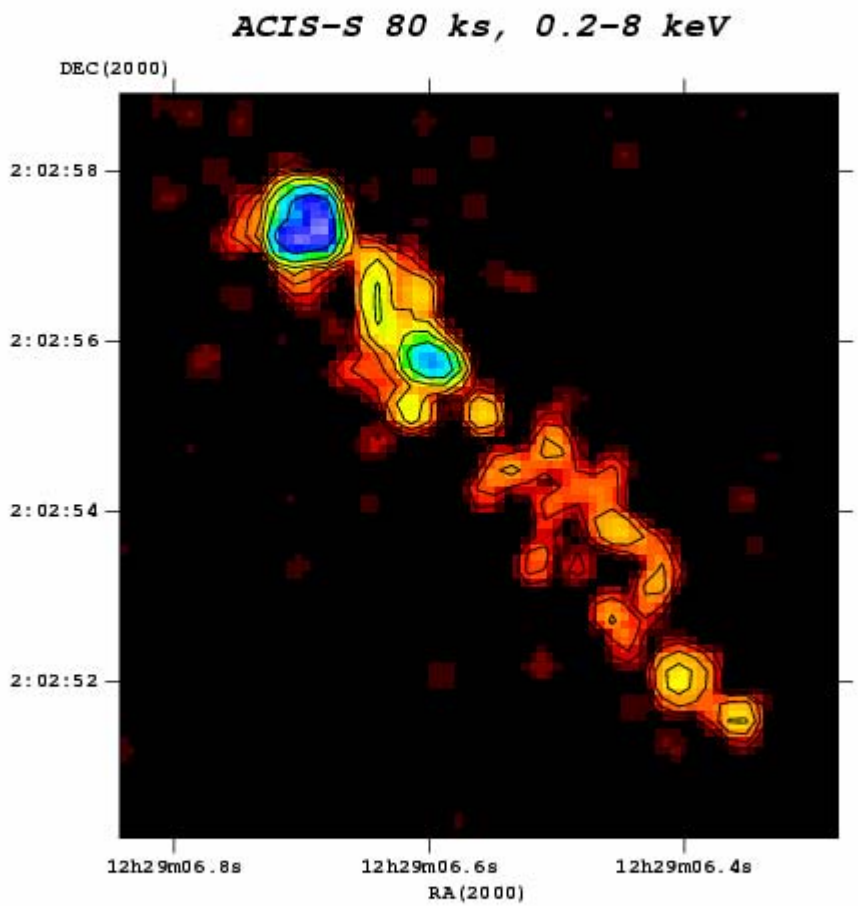

Jet in radiogalaxy

IC 4296 at 20 cm with 3.2” resolution.

10” is about 2 kps.

VLA, Killeen et al. (1986)

Total extent is about

400 kpc

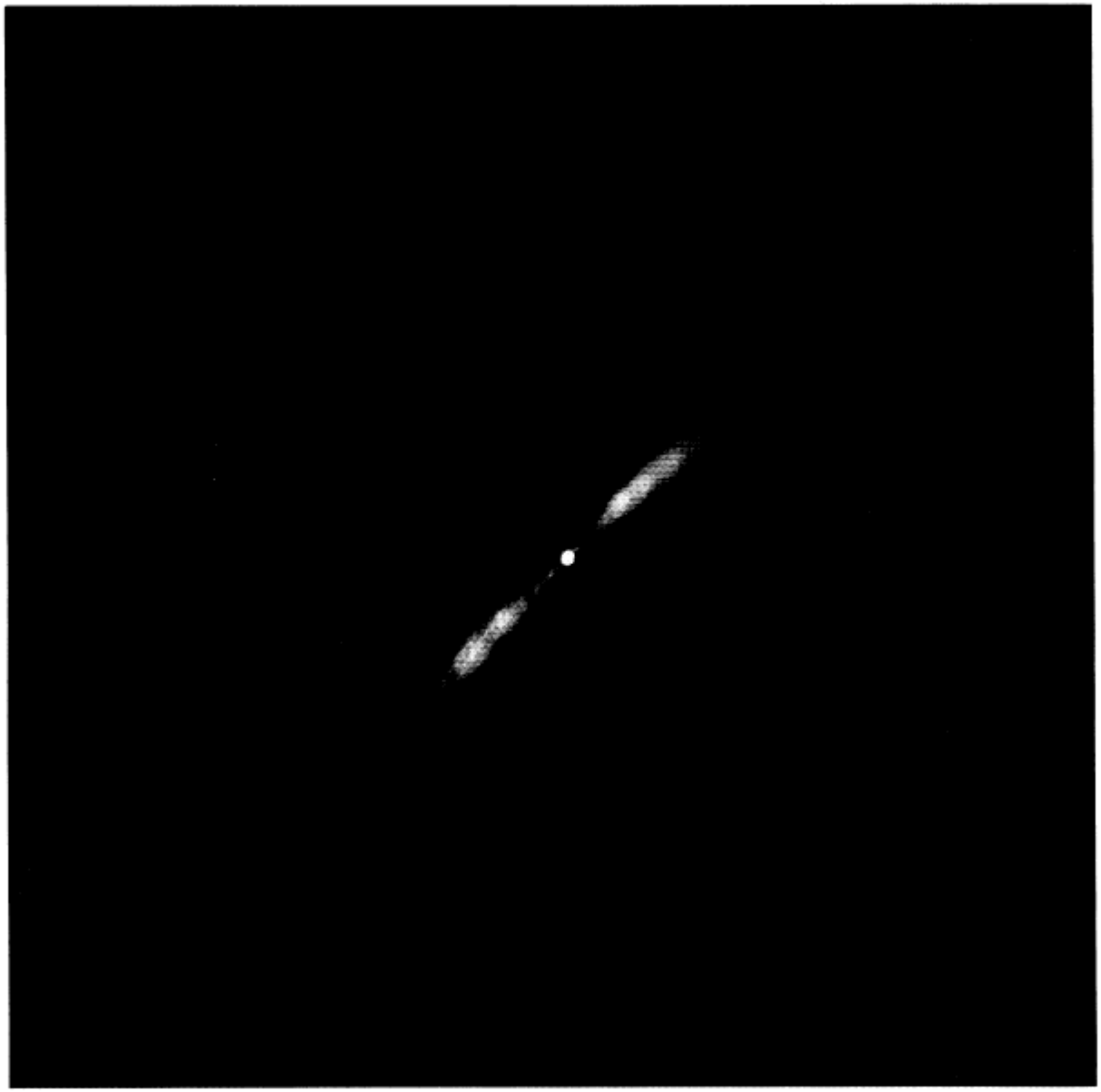

FIG. 11.—Radiograph of the jets at 20 cm with 3.″2 resolution

W.A.Hiltner
ApJ, 1959

PHOTOELECTRIC POLARIZATION OBSERVATIONS OF THE JET IN M87*

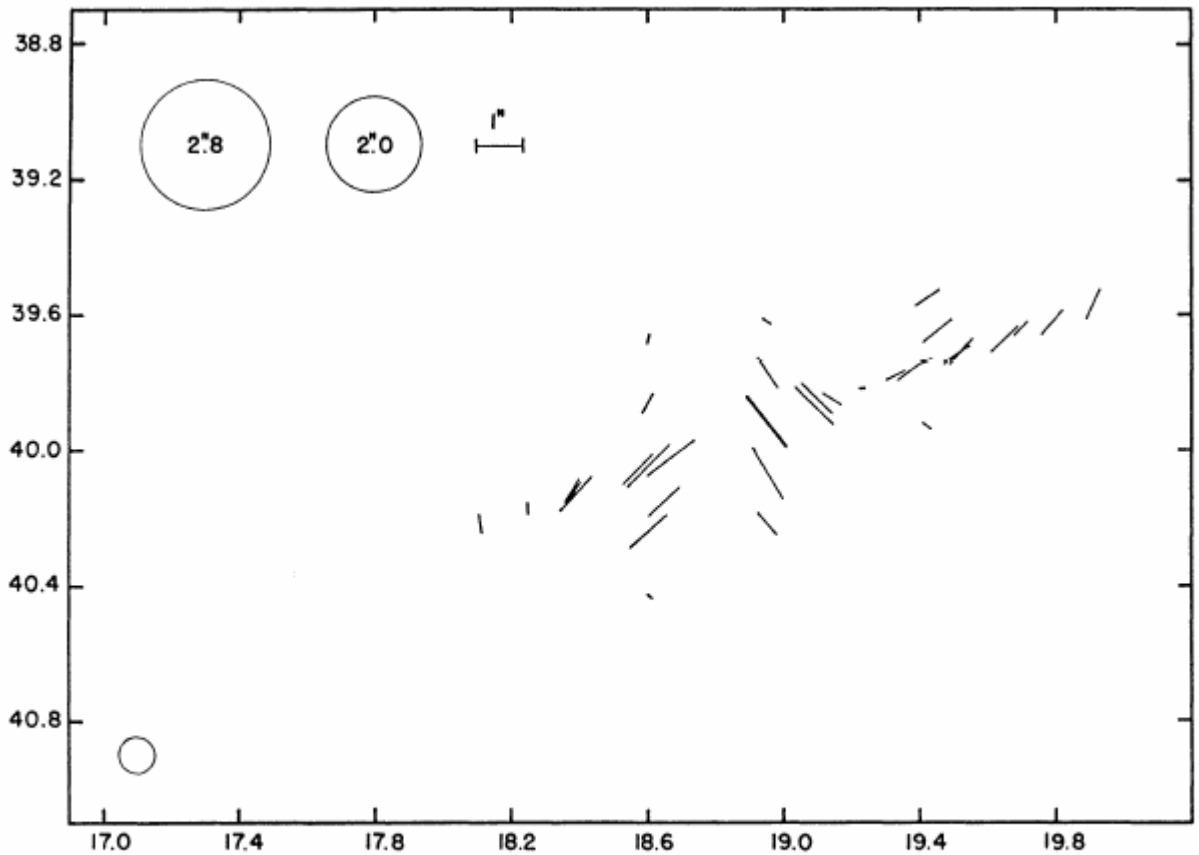

FIG. 1.—Polarization observations of M87. The co-ordinates refer to the observed position relative to a guide star. All lines refer to individual observations except the heavy one, which is the mean of ten observations. The relative sizes of the diaphragms used are shown in the upper left of the figure. The position of the nucleus of M87 is shown by a small open circle in the lower left.

Jet in M87:

radio, 14GHz, **VLA**, 0.2”

HST (F814W)

Chandra image, 0.2”,

0.2-8 keV

Adaptively smoothed

Chandra image

Marshall et al. (2001)

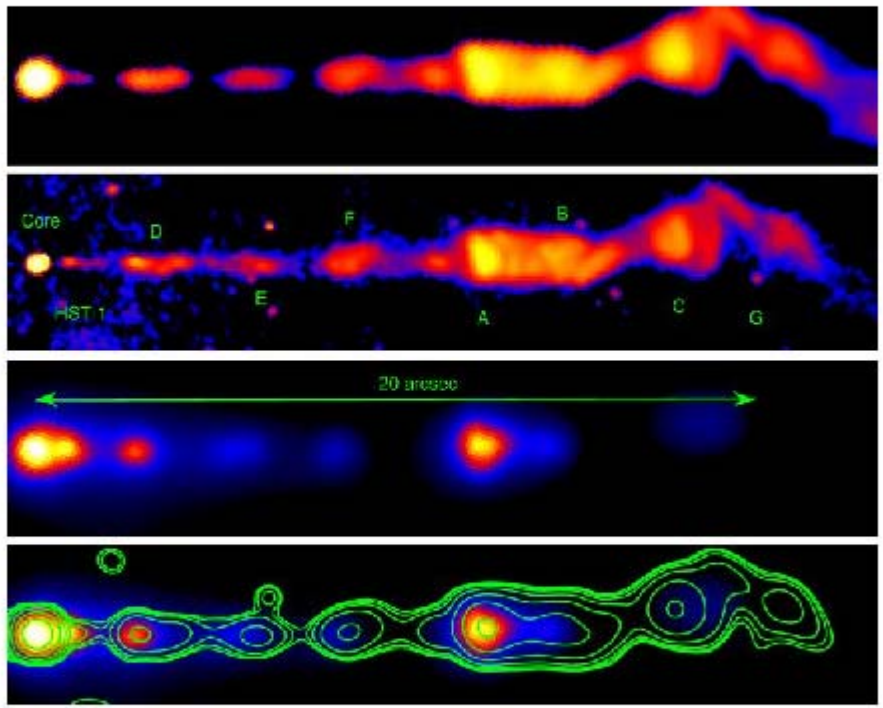

Fig. 1.— Images of the jet in M 87 in three different bands, rotated to be horizontal, and an overlay of optical contours over the X-ray image. *Top:* Image at 14.435 GHz using the VLA. The spatial resolution is about 0.2″. *Second panel:* The *Hubble* Space Telescope Planetary Camera image in the F814W filter from Perlman et al. (2001a). The brightest knots are labelled according to the nomenclature used by Perlman et al. (2001a) and others. *Third panel:* Adaptively smoothed *Chandra* image of the X-ray emission from the jet of M 87 in 0.20″ pixels. The X-ray and optical images have been registered to each other to about 0.05″ using the position of the core. *Fourth panel:* Smoothed *Chandra* image overlaid with contours of a Gaussian smoothed version of the HST image, designed to match the *Chandra* point response function. The X-ray and optical images have been registered to each other to

It is convenient sometimes to investigate jets in a simple model of infinitely long circular cylinder (Chandrasekhar and Fermi, 1953). Magnetic fields in collimated jets is determining its direction, and axial current is stabilizing its elongated form at large distances from the source (AGN). When observed with high angular resolution these jets show structure with bright knots separated by relatively dark regions. High percentages of polarization, sometimes more then 50% in some objects, indicates the nonthermal nature of the radiation which is well explained as the synchrotron radiation of the relativistic electrons in a weak but ordered magnetic field.

It was assumed by Bisnovatyi-Kogan, Komberg, Fridman (1969); that jets are formed by a sequence of outbursts from the nucleus with considerable charge separation at the moment of the outburst. The direction of motion the outburst is determined by the large-scale magnetic field. The outburst are accompanied by an intense electromagnetic disturbance which propagates outward moving with the jet material in the direction of the large scale magnetic field. It was suggested also that a toroidal magnetic field, generated during the outbursts is important for the lateral confinement of of the jet.

Long-periodic proper oscillations in the plasma cylinder with a finite radius, and emission of electromagnetic waves had been studied by Bisnovatyi-Kogan and Lovelace (1995). Enhanced oscillations in such cylinder have been studied by Bisnovatyi-Kogan (2004).

Cylinder with oscillating current

$$\operatorname{div}\mathbf{B}=0, \quad \operatorname{rot}\mathbf{B}=\frac{1}{c}\frac{\partial\mathbf{E}}{\partial t}+\frac{4\pi}{c}\mathbf{j},$$

$$\operatorname{rot}\mathbf{E}=-\frac{1}{c}\frac{\partial\mathbf{B}}{\partial t}, \quad \operatorname{div}\mathbf{E}=4\pi\rho_{\boldsymbol{e}}.$$

For periodic oscillations with all values $\sim \exp(-i\omega t)$ they read

$$\operatorname{div}\mathbf{B}=0, \ \operatorname{rot}\mathbf{B}=-\frac{i\omega}{c}\mathbf{E}+\frac{4\pi}{c}\mathbf{j}, \ \operatorname{rot}\mathbf{E}=\frac{i\omega}{c}\mathbf{B}, \ \operatorname{div}\mathbf{E}=0.$$

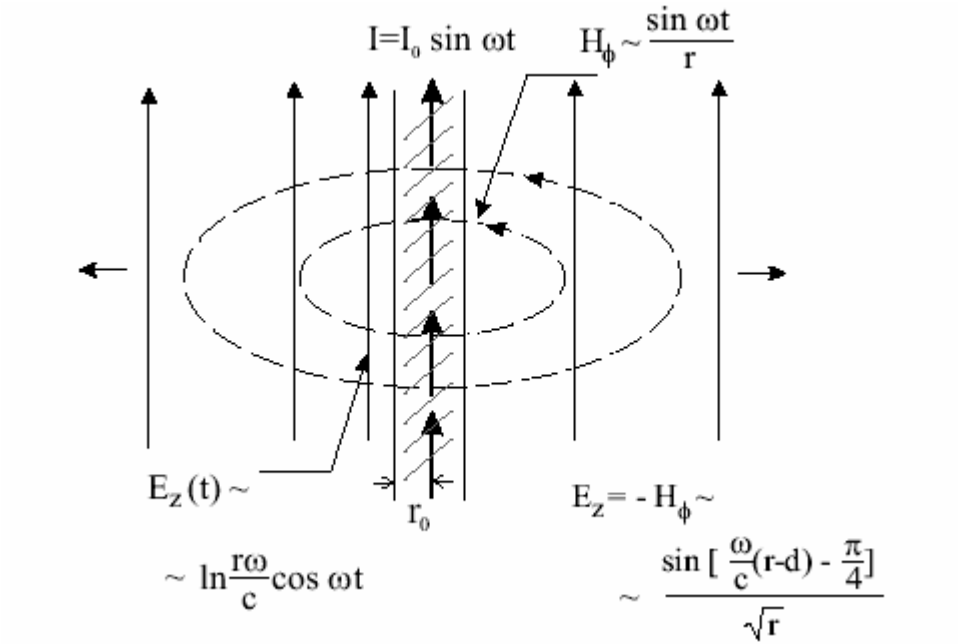

Magnetic and electrical fields around the infinite cylinder with the radius **r_0**, and low-frequency sinusoidal electrical current along the cylinder axis.
In the near zone electrical and magnetic fields are varying in antiphase,
and far from the cylinder the expanding cylindrical electromagnetic wave is formed,
with **E_z=-B_phi**

In the cylinder the only nonzero components are

$$\text{are } E_z,\ B_\phi,\ j_z, \text{ and } \partial/\partial\phi = \partial/\partial z = 0.$$

To find the electromagnetic field around the cylinder with oscillating cullent it is necessary solve one equation

$$\frac{1}{r}\frac{d}{dr}\left(r\frac{dE_z}{dr}\right) + \frac{\omega^2}{c^2}E_z + \frac{4\pi i\omega}{c^2}j_z = 0.$$

The solution is obtained analytically for long waves, $\lambda > R$ (radius of the cylinder), Bisnovatyi-Kogan (2004).

1. Vacuum solution for the expanding wave (outer boundary condition.
2. Solution inside the cylinder.
3. Matching of solutions in absence of surface currents and electrical charges.

The solution for long-wave oscilaltions is

$$E_z = \frac{\pi\omega}{c^2} I_0^{(i)} [Y_0(x)\cos\omega t - J_0(x)\sin\omega t],$$

$$B_\phi = -\frac{\pi\omega}{c^2} I_0^{(i)} [Y_1(x)\sin\omega t + J_1(x)\cos\omega t].$$

Here the total current through the cylinder is taken as

$$I_0 = I_0^{(r)}\cos\omega t + I_0^{(i)}\sin\omega t,$$

with $I_0^{(r)}$=0.

In the near zone (in antiphase): $E_z = \frac{2\omega}{c^2} I_0^{(i)} \ln \frac{r\omega}{2c} \cos \omega t,$

$$B_\phi = \frac{2I_0^{(i)}}{cr} \sin \omega t.$$

In the wave zone (in phase):

$$B_\phi = -E_z = -\frac{1}{c}\sqrt{\frac{2\pi\omega}{cr}} I_0^{(i)} \sin[\frac{\omega}{c}(r - ct) - \frac{\pi}{4}].$$

Electromagnetic energy flux F from the cylinder withlength **l**, and radius **r** (Poynting flux):

$$F = \frac{\pi^3}{2} e^2 l r_0^4 \omega n_e^2 \approx 2 \cdot 10^{49}\,\mathrm{erg/s}\, \frac{l}{1\,\mathrm{kpc}} \left(\frac{r_0}{1\,\mathrm{pc}}\right)^4 \frac{100\,\mathrm{yr}}{T} \left(\frac{n_e}{10^{-10}\,\mathrm{cm}^{-3}}\right)^2$$

Generation of strong electromagnetic wave by proper oscillations in a separate blob, Bisnovatyi-Kogan and Lovelace (1995).

Linear non-potential oscillations had been investigated, heavy ions, charge separation, long waves, low frequency branch.

Conclusions

1. Nonpotential oscillations induced by initial charge separation in the expelling blob, produce a strong electromagnetic wave carring large energy flux and accelerating particles up to very high energies, far from the nucleus.

2. Similarity of the acceleration mechanisms of the particles in the **pulsars** and **relativistic jets** could be a reason of the similarity of the high energy radiation around 100 Mev, which had been observed by EGRET in number of **radiopulsars, quasars and AGN**.